

Combining Mixed Effects Hidden Markov Models with Latent Alternating Recurrent Event Processes to Model Diurnal Active-Rest Cycles

Benny Ren

Department of Biostatistics, Epidemiology, and Informatics,
University of Pennsylvania, Philadelphia, U.S.A.
email: bennyren@pennmedicine.upenn.edu

and

Ian Barnett

Department of Biostatistics, Epidemiology, and Informatics,
University of Pennsylvania, Philadelphia, U.S.A.
email: ibarnett@pennmedicine.upenn.edu

SUMMARY: Data collected from wearable devices and smartphones can shed light on an individual's patterns of behavior and circadian routine. Phone use can be modeled as alternating between the state of active use and the state of being idle. Markov chains and alternating recurrent event models are commonly used to model state transitions in cases such as these, and the incorporation of random effects can be used to introduce time-of-day effects. While state labels can be derived prior to modeling dynamics, this approach omits informative regression covariates that can influence state memberships. We instead propose a recurrent event proportional hazards (PH) regression to model the transitions between latent states. We propose an Expectation-Maximization (EM) algorithm for imputing latent state labels and estimating regression parameters. We show that our E-step simplifies to the hidden Markov model (HMM) forward-backward algorithm, allowing us to recover a HMM in addition to PH models. We derive asymptotic distributions for our model parameter estimates and compare our approach against competing methods through simulation as well as in a digital phenotyping study that followed smartphone use in a cohort of adolescents with mood disorders.

KEY WORDS: Alternating Recurrent Event Processes; Expectation Maximization Algorithm; Hidden Markov Models; Latent Variable Modeling; Longitudinal data; mHealth

1. Introduction

Diurnal and circadian rhythm studies often model physiological processes as periodic cycles, such as a person's active and rest cycles. Sleep and diurnal rhythm are essential components of many circadian physiological processes with a clear time-of-day effect on active and rest cycles (Melo et al., 2017; Skarke et al., 2017; Morris et al., 2012; Lange et al., 2010). While classification of physiological processes is an ongoing area of research, in many instances processes can be discretized into a few state categories such as active and rest state labels (Qi et al., 2018). Here we consider this problem of estimating an individual's cycles between rest and active states in a mobile health (mHealth) setting, based on wearable device or smartphone sensor data. If the true state labels are known, then a Markov chain can be used to model state transitions over time, otherwise a hidden Markov model (HMM) can be used to simultaneously perform classification and state transition estimation (Langrock et al., 2013; Pan et al., 2012; Song et al., 2015; Huang et al., 2018). In addition, HMM models have been extended to incorporate time-of-day effects as periodicity or seasonality using random effects (Stoner and Economou, 2020; Maruotti and Rocci, 2012; Holsclaw et al., 2017; Altman, 2007). Continuous-time hidden Markov models (CT-HMM) have also been used for state classification in similar contexts (Liu et al., 2015; Bureau et al., 2003; Jackson et al., 2003).

It's important to note that active and rest state transitions are ergodic processes and the sojourn time between these states can be modeled with a proportional hazards (PH) regression in both directions, active-to-rest and rest-to-active. These two directions of transitions can be viewed as an alternating recurrent event PH model (Shinohara et al., 2018; Wang et al., 2020). Already, hazard rates have been incorporated into continuous-time Markov chains (CTMC) to model sojourn times (Weedon-Fekjær et al., 2008; Hubbard et al., 2016). However, the ability for alternating recurrent event processes to accurately model sojourn

times has not yet been paired with the ability of HMMs to jointly estimate the underlying latent states.

We propose an approach that takes advantage of the strengths of both HMMs and alternating recurrent event models to jointly estimate latent states while simultaneously providing flexible modeling of sojourn times. Our Expectation-Maximization (EM) algorithm imputes latent active and rest state labels while modeling state transitions with an alternating recurrent event process using exponential PH regressions (Dempster et al., 1977). Under the EM algorithm, we show that the E-step in this case simplifies to imputations involving a HMM forward-backward algorithm where state transition probabilities are defined as logistic regression probabilities (Baum et al., 1970; Altman, 2007). We also show that the M-step reduces to PH models weighted by E-step imputations, which allows us to conveniently incorporate time-of-day random intercepts to model diurnal rhythm and derive large sample theory inference. Furthermore, informative regression covariates, often omitted in state labeling, are incorporated into the latent state imputation using the EM algorithm.

We apply this approach to estimate individual-level active-rest cycles in a sample of patients with affective disorders from their passively collected smartphone sensor data, namely through the accelerometer and screen on/off data of patient smartphones. We are able to quantify the strength of a patient's routine by equating the magnitude of time-of-day random intercepts with the strength of a patient's diurnal rhythms. This quantification of the strength of routine can be correlated with a myriad of relevant clinical outcomes, as the regularity of diurnal rhythms plays an important role in psychopathology, with past studies having shown associations between irregular rhythms and adverse health outcomes (Monk et al., 1990, 1991; Shear et al., 1994; Jones et al., 2006; Alloy et al., 2015; Lyall et al., 2018).

The rest of this manuscript is organized as follows. In Section 2, we introduce the data and derive the EM algorithm for estimating the alternating recurrent event exponential PH model

and the accompanying HMM. In Section 3, we compare our alternating recurrent event model and HMM with competing approaches through simulation and also by estimating active/rest cycles using smartphone data in a cohort of patients with affective disorders.

2. Methods

2.1 Data

Our data consist of n_I individuals, each individual having n_{iJ} sequences of data to be modeled with separate hidden Markov models, and we consider the j th sequence of data to have n_{ijK} transitions in the corresponding HMM. Multiple sequences of data for a single individual occur when there are large gaps of missing data during the course of follow-up, in which case each continuous data segment is modeled with a different HMM. The j th HMM of the i th individual has $n_{ijK} + 1$ active or rest states $\mathbf{A} = \{A(t_{ij0}), A(t_{ij1}), \dots, A(t_{ijn_{ijK}})\}$, where hourly time-stamps t_{ijk} are increasing in k . We denote active and rest states as $A(t_{ijk}) = 1$ and $A(t_{ijk}) = 2$ respectively, with an outline of our HMM in Figure 1.

Within each sequence of data, we define event times to state transitions $h_{ijk} = t_{ijk} - t_{ij(k-1)}$, which follow from an exponential distribution. In practice, if a sequence contain a value of h_{ijk} that is large (e.g., greater than 24 hours), simply break up the sequence into multiple smaller sequences around that h_{ijk} in order to ensure that at most a single transition occurs for each h_{ijk} . Small values of h_{ijk} can be obtained in high frequency data collection settings such as mHealth studies. Furthermore, recurrent exponential PH models are analogous with a non-homogeneous Poisson point processes which retains the memoryless property, allowing us to chain multiple transitions together. The covariate used in the exponential PH regression are average acceleration magnitudes (Euclidean norm) from the preceding hour evaluated at n_{ijK} transitions and are outlined in Figure 1. We denote the intercept and covariates as vectors $\mathbf{X}_{ij} = \{\mathbf{x}(t_{ij1}), \mathbf{x}(t_{ij2}), \dots, \mathbf{x}(t_{ijn_{ijK}})\}$. We make an ergodic state transition assumption where

states will inevitably communicate with each other, e.g., the active-to-rest and rest-to-active transitions will eventually occur. Therefore, the survival function captures the likelihood contribution when a state transition did not occur, meaning the transition will occur at some future time.

Because we do not have the true state labels \mathbf{A} , we rely on state dependent observations. We use screen-on counts for each hour $\mathbf{y}_{ij} = \{Y(t_{ij0}), Y(t_{ij1}), \dots, Y(t_{ijn_{ijK}})\}$ as observations from state dependent distributions $Y(t_{ijk}) | \{A(t_{ijk}) = s\} \sim \text{Poisson}(\mu_s)$, where $s \in \{1, 2\}$ and μ_s are state specific parameters.

[Figure 1 about here.]

2.2 Alternating Recurrent Event PH Model

In our two state setting, rates of transition from state s to the other state are defined as $\lambda_s(t_{ijk}) = \exp(\mathbf{x}^\top(t_{ijk})\boldsymbol{\beta}_s)$. For example, $\lambda_1(t_{ijk})$ denotes the rate of transition from state 1-to-2 (active-to-rest). Alternating recurrent event PH models often need to account for longitudinal nature of the data, i.e., repeated measurements. Mixed effects or frailties can be used to account for the recurrent nature of the data (Wang et al., 2020; McGilchrist and Aisbett, 1991; Ripatti and Palmgren, 2000; Abrahantes et al., 2007). Modifying the standard exponential PH model with a shared log-normal frailties or normally distributed random intercepts, state transition hazards become $\lambda_s(t_{ijk}) = \exp(\eta_s(t_{ijk})) = \exp(\mathbf{x}^\top(t_{ijk})\boldsymbol{\beta}_s + \mathbf{z}^\top(t_{ijk})\mathbf{b}_s)$, where $\mathbf{b}_s \sim N(\mathbf{0}, \sigma_s^2 \mathbf{I})$ and $\mathbf{z}^\top(t_{ijk})$ are one-hot vectors designed to toggle the appropriate random intercepts within $\{\mathbf{b}_1, \mathbf{b}_2\}$.

We are interested in understanding the effect of hour of the day has on state transition and membership. By fitting an hour-of-day random intercepts, then \mathbf{b}_1 and \mathbf{b}_2 are each of length 24 and $[\mathbf{z}(t_{ijk})]_r = 1$ only if t_{ijk} is in the r th hour of the day. The random intercept variances σ_1^2 and σ_2^2 are the test statistics in a mixed effect ANOVA, where the null hypothesis has the interpretation of hour-of-day having no effect on state transitions. In other words large

values of $\sigma_1^2 + \sigma_2^2$ lead to rejecting the null and estimates of $\sigma_1^2 + \sigma_2^2$ serve as a quantification of the regularity of diurnal rhythms, strength of hour-of-day effects on active and rest state transitions. Despite our usage of the random effect structure to represent time-of-day, this formulation can be used more generally with $\mathbf{z}^\top(t_{ijk})$ being fixed or time varying.

Our model parameters are expressed through the complete data likelihood

$$\begin{aligned} L(\boldsymbol{\beta}_1, \mathbf{b}_1, \sigma_1^2, \boldsymbol{\beta}_2, \mathbf{b}_2, \sigma_2^2, \mu_1, \mu_2 | \mathbf{A}) &= \left[\prod_{s=1}^2 L(\boldsymbol{\beta}_s, \sigma_s^2, \mathbf{b}_s | \mathbf{A}) \right] L(\mu_1, \mu_2 | \mathbf{A}) \\ &= \left[\prod_{s=1}^2 L(\boldsymbol{\beta}_s | \mathbf{A}, \mathbf{b}_s) f(\mathbf{b}_s | \sigma_s^2) \right] L(\mu_1, \mu_2 | \mathbf{A}) \end{aligned} \quad (1)$$

where \mathbf{A} are the true state labels. The two PH likelihoods for state transitions are given as

$$L(\boldsymbol{\beta}_s | \mathbf{A}, \mathbf{b}_s) f(\mathbf{b}_s | \sigma_s^2) = \left[\prod_{i=1}^{n_I} \prod_{j=1}^{n_{iJ}} \prod_{k=1}^{n_{ijk}} [f(h_{ijk} | \lambda_s(t_{ijk}))]^{d_s(t_{ijk})} [S(h_{ijk} | \lambda_s(t_{ijk}))]^{c_s(t_{ijk})} \right] f(\mathbf{b}_s | \sigma_s^2)$$

where $f(h_{ijk} | \lambda_s(t_{ijk})) = \lambda_s(t_{ijk}) \exp(-\lambda_s(t_{ijk})h_{ijk})$ and $S(h_{ijk} | \lambda_s(t_{ijk})) = \exp(-\lambda_s(t_{ijk})h_{ijk})$ are derived from the exponential distribution. We denote indicators for state 1-to-2 transition, $d_1(t_{ijk}) = \mathbb{1}[A(t_{jk-1}) = 1, A(t_{ijk}) = 2]$, as $\mathbf{d}_1 = \{d_1(t_{111}), d_1(t_{112}), \dots, d_1(t_{ijk}), \dots\}$ and a 2-to-1 transition as \mathbf{d}_2 . We interpret failure to transition out of state 1, $c_1(t_{ijk}) = \mathbb{1}[A(t_{ij(k-1)}) = 1, A(t_{ijk}) = 1]$, as censoring, denoted as $\mathbf{c}_1 = \{c_1(t_{111}), c_1(t_{112}), \dots, c_1(t_{ijk}), \dots\}$ and we similarly define \mathbf{c}_2 . The screen-on count state conditional Poisson likelihoods is given as $L(\mu_1, \mu_2 | \mathbf{A}) = \prod_{i=1}^{n_I} \prod_{j=1}^{n_{iJ}} \prod_{k=0}^{n_{ijk}} \prod_{s=1}^2 f(y(t_{ijk}) | \mu_s)^{u_s(t_{ijk})}$, where state memberships \mathbf{u} , are denoted as indicators $u_s(t_{ijk}) = \mathbb{1}[A(t_{ijk}) = s]$. However, since the true labels of $A(t_{ijk})$ are unknown, \mathbf{d}_s , \mathbf{c}_s , and \mathbf{u} are latent variables and (1) becomes a mixture model.

2.3 EM Algorithm for PH Regression and HMM Parameters

The log-likelihood of (1) are linear functions of \mathbf{d}_s , \mathbf{c}_s , and \mathbf{u} , lending our optimization approach to an EM algorithm (Dempster et al., 1977; Baum et al., 1970). Through the EM algorithm, indicators \mathbf{d}_s , \mathbf{c}_s , and \mathbf{u} are imputed as continuous probabilities, in the process of obtaining maximum likelihood estimates (MLEs). As a result, the alternating recurrent event exponential PH model reduces to two weighted frailty models (Rondeau et al., 2012; Munda

et al., 2012; Balan and Putter, 2019; Monaco et al., 2018). We denote PH model weights as $\mathbf{w}(t_{ijk}) = \{c_1(t_{ijk}), d_1(t_{ijk}), c_2(t_{ijk}), d_2(t_{ijk})\}$, which belong to a 4-dimensional probability simplex, i.e., values are non-negative and $\|\mathbf{w}(t_{ijk})\|_1 = 1$. Poisson mixture model weights $\mathbf{u}(t_{ijk}) = \{u_1(t_{ijk}), u_2(t_{ijk})\}$ belong to a 2-dimensional probability simplex. A general EM algorithm can be found in Chapter 4 of Zucchini et al. (2017), while our EM algorithm iteratively estimates the weights $\mathbf{w}(t_{ijk})$ and $\mathbf{u}(t_{ijk})$ using the forward-backward algorithm of Baum et al. (1970) and $\{\boldsymbol{\beta}_1, \mathbf{b}_1, \sigma_1^2, \boldsymbol{\beta}_2, \mathbf{b}_2, \sigma_2^2\}$ using survival modeling.

2.3.1 E-step. In the E-step, we derive the expectation of $\mathbf{w}(t_{ijk})$ conditional on model parameters and all data in the ij th HMM denoted by \mathbf{y}_{ij} and \mathbf{X}_{ij}

$$\begin{aligned}\mathbb{E}[d_1(t_{ijk})|\mathbf{y}_{ij}, \mathbf{X}_{ij}, \Theta_{ij}] &= \Pr(A(t_{ij(k-1)}) = 1, A(t_{ijk}) = 2|\mathbf{y}_{ij}, \mathbf{X}_{ij}, \Theta_{ij}) \\ &= \left(\frac{\alpha_1(t_{ij(k-1)})\nu_2(t_{ijk})}{\Pr(\mathbf{Y}_{ij} = \mathbf{y}_{ij}|\mathbf{X}_{ij}, \Theta_{ij})} \right) \frac{f(h_{ijk}|\lambda_1(t_{ijk}))}{f(h_{ijk}|\lambda_1(t_{ijk}))+S(h_{ijk}|\lambda_1(t_{ijk}))} \\ \mathbb{E}[c_1(t_{ijk})|\mathbf{y}_{ij}, \mathbf{X}_{ij}, \Theta_{ij}] &= \Pr(A(t_{ij(k-1)}) = 1, A(t_{ijk}) = 1|\mathbf{y}_{ij}, \mathbf{X}_{ij}, \Theta_{ij}) \\ &= \left(\frac{\alpha_1(t_{ij(k-1)})\nu_1(t_{ijk})}{\Pr(\mathbf{Y}_{ij} = \mathbf{y}_{ij}|\mathbf{X}_{ij}, \Theta_{ij})} \right) \frac{S(h_{ijk}|\lambda_1(t_{ijk}))}{f(h_{ijk}|\lambda_1(t_{ijk}))+S(h_{ijk}|\lambda_1(t_{ijk}))}\end{aligned}$$

where $\Theta_{ij} = \{\boldsymbol{\delta}_{ij}, \boldsymbol{\beta}_1, \mathbf{b}_1, \sigma_1^2, \boldsymbol{\beta}_2, \mathbf{b}_2, \sigma_2^2\}$, $\alpha_1(t_{ijk}) \propto \Pr(A(t_{ijk}) = 1|y_{ij0}, \dots, y_{ijk}, \mathbf{x}_{ij1}, \dots, \mathbf{x}_{ijk}, \Theta_{ij})$ and $\nu_1(t_{ijk}) \propto \Pr(A(t_{ijk}) = 1|y_{ijk}, \dots, y_{ijn_{ijK}}, \mathbf{x}_{ij(k+1)}, \dots, \mathbf{x}_{ijn_{ijK}}, \Theta_{ij})$ are forward and backward probabilities of a HMM. Vectors $\boldsymbol{\delta}_{ij}$ are of initial state distribution probabilities for the ij th HMM. The transition probability matrix $\boldsymbol{\Gamma}(t_{ijk})$, derived by normalizing the alternating recurrent event exponential PH models are

$$\boldsymbol{\Gamma}(t_{ijk}) = \begin{bmatrix} \gamma_{11}(t_{ijk}) & \gamma_{12}(t_{ijk}) \\ \gamma_{21}(t_{ijk}) & \gamma_{22}(t_{ijk}) \end{bmatrix} = \begin{bmatrix} 1 - \text{expit}(\eta_1(t_{ijk})) & \text{expit}(\eta_1(t_{ijk})) \\ \text{expit}(\eta_2(t_{ijk})) & 1 - \text{expit}(\eta_2(t_{ijk})) \end{bmatrix}$$

where $f(h_{ijk}|\lambda_s(t_{ijk}))/[f(h_{ijk}|\lambda_s(t_{ijk}))+S(h_{ijk}|\lambda_s(t_{ijk}))] = [1 + \exp(-\eta_s(t_{ijk}))]^{-1} = \text{expit}(\eta_s(t_{ijk}))$. The weights from $\mathbf{w}(t_{ijk})$ can more generally be written as

$\Pr(A(t_{ij(k-1)}) = q, A(t_{ijk}) = r|\mathbf{y}_{ij}, \mathbf{X}_{ij}, \Theta_{ij}) \propto \alpha_q(t_{ij(k-1)})\nu_r(t_{ijk})\gamma_{qr}(t_{ijk})$. The E-step involves imputing $\mathbf{w}(t_{ijk})$ through a HMM, using a forward-backward algorithm, where transition probabilities are standard logistic functions (Baum et al., 1970; Zucchini et al., 2017).

We denote forward and backward probabilities vectors $\boldsymbol{\alpha}^\top(t_{ijk}) = \boldsymbol{\delta}_{ij}\mathbf{P}(t_{ij0}) \prod_{m=1}^k \boldsymbol{\Gamma}(t_{ijm})\mathbf{P}(t_{ijm})$ and $\boldsymbol{\nu}(t_{ijk}) = \mathbf{P}(t_{ijk}) \prod_{m=k+1}^{n_{ijk}} \boldsymbol{\Gamma}(t_{ijm})\mathbf{P}(t_{ijm})\mathbf{1}$, where state dependent distribution are contained in the 2×2 diagonal matrix $\mathbf{P}(t_{ijk}) = \text{diag}\left(f(y(t_{ijk})|\mu_1), f(y(t_{ijk})|\mu_2)\right)$. Note that $\Pr(\mathbf{Y}_{ij} = \mathbf{y}_{ij} | \mathbf{X}_{ij}, \Theta_{ij}) = \boldsymbol{\alpha}^\top(t_{ijk})\boldsymbol{\Gamma}(t_{ijk})\boldsymbol{\nu}(t_{ij(k+1)})$, and are used to normalize E-step probabilities. The E-step update for iteration $l + 1$, simplifies to calculating probabilities $\mathbf{w}^{(l+1)}(t_{ijk})$ as

$$\begin{bmatrix} c_1^{(l+1)}(t_{ijk}) & d_1^{(l+1)}(t_{ijk}) \\ d_2^{(l+1)}(t_{ijk}) & c_2^{(l+1)}(t_{ijk}) \end{bmatrix} \propto \left[\boldsymbol{\alpha}^\top(t_{ij(k-1)}) \otimes \boldsymbol{\nu}^{(l)}(t_{ijk}) \right] \odot \boldsymbol{\Gamma}^{(l)}(t_{ijk})$$

such that the sum of all elements is equal to one, $\|\mathbf{w}^{(l+1)}(t_{ijk})\|_1 = 1$. Operations \otimes and \odot are Kronecker and Hadamard products respectively. Similarly, the update for the Poisson mixture model weights are $\mathbf{u}^{(l+1)}(t_{ijk}) \propto \boldsymbol{\alpha}^{(l)}(t_{ijk}) \odot \left[\boldsymbol{\Gamma}^{(l)}(t_{ij(k+1)})\boldsymbol{\nu}^{(l)}(t_{ij(k+1)}) \right]$, such that $\|\mathbf{u}^{(l+1)}(t_{ijk})\|_1 = 1$. The E-step update can be computed quickly in parallel where each ijk th HMM is processed independently.

2.3.2 M-step. The M-step update for $\{\mu_1^{(l+1)}, \mu_2^{(l+1)}\}$ involves solving the mixture model $L(\mu_1, \mu_2 | \mathbf{u}^{(l+1)}) = \prod_{i=1}^{n_I} \prod_{j=1}^{n_{iJ}} \prod_{k=0}^{n_{ijk}} \prod_{s=1}^2 f(y(t_{ijk})|\mu_s)^{u_s^{(l+1)}(t_{ijk})}$, where solutions are known for most distributions and $\mu_s^{(l+1)} = \left(\sum_{ijk} u_s^{(l+1)}(t_{ijk})\right)^{-1} \left(\sum_{ijk} u_s^{(l+1)}(t_{ijk})y(t_{ijk})\right)$ in the Poisson setting. From $\{\mu_1^{(l+1)}, \mu_2^{(l+1)}\}$, we have updates $\mathbf{P}^{(l+1)}(t_{ijk})$.

The update for $\{\boldsymbol{\beta}_s^{(l+1)}, \mathbf{b}_s^{(l+1)}, \sigma_s^{2(l+1)}\}$ involves fitting two frailty models for $L(\boldsymbol{\beta}_s, \sigma_s^2, \mathbf{b}_s | \mathbf{c}_s^{(l+1)}, \mathbf{d}_s^{(l+1)})$ which can be accomplished by recognizing $\{\mathbf{d}_s^{(l+1)}, \mathbf{c}_s^{(l+1)}\}$ as log-likelihood weights or case weights. We duplicate each row of data to be both a transition event and a censored outcome and then weight the rows by $\mathbf{d}_s^{(l+1)}$, and $\mathbf{c}_s^{(l+1)}$ respectively. A data augmentation example is outlined in Table 1.

[Table 1 about here.]

While there are numerous survival packages in R, we need a package that can incorporate weights, parametric PH models and normally distributed random intercepts (Therneau

and Lumley, 2015). The R package `tramME` can be used to fit our weighted exponential parametrization of shared log-normal frailty models (Tamási and Hothorn, 2021). The package `tramME` uses a *most likely transformations* approach combined with an efficient implementation of the Laplace approximation to fit the shared log-normal frailty models (Hothorn et al., 2018; Hothorn, 2020; Kristensen et al., 2016). By updating $\{\boldsymbol{\beta}_1^{(l+1)}, \mathbf{b}_1^{(l+1)}, \boldsymbol{\beta}_2^{(l+1)}, \mathbf{b}_2^{(l+1)}\}$ we also obtain updates for our transition rates, $\lambda_1^{(l+1)}(t_{ijk})$ and $\lambda_2^{(l+1)}(t_{ijk})$ which are used to calculate transition probabilities $\boldsymbol{\Gamma}^{(l+1)}(t_{ijk})$.

The M-step updates for the initial state distribution are $\boldsymbol{\delta}_{ij}^{(l+1)} \propto [\boldsymbol{\delta}_{ij}^{(l)} \mathbf{P}^{(l+1)}(t_{ij0})] \odot [\boldsymbol{\Gamma}^{(l+1)}(t_{ij1}) \boldsymbol{\nu}^{(l+1)}(t_{ij1})]$, such that $\|\boldsymbol{\delta}_{ij}^{(l+1)}\|_1 = 1$. Finally, we iteratively calculate the E-step: $\{\mathbf{w}^{(l+1)}(t_{ijk}), \mathbf{u}^{(l+1)}(t_{ijk})\}$, and M-step: $\{\boldsymbol{\delta}_{ij}^{(l+1)}, \boldsymbol{\beta}_1^{(l+1)}, \mathbf{b}_1^{(l+1)}, \sigma_1^{2(l+1)}, \boldsymbol{\beta}_2^{(l+1)}, \mathbf{b}_2^{(l+1)}, \sigma_2^{2(l+1)}\}$ until convergence to obtain the maximum likelihood estimate of $\{\boldsymbol{\beta}_1, \mathbf{b}_1, \sigma_1^2, \boldsymbol{\beta}_2, \mathbf{b}_2, \sigma_2^2\}$.

2.4 EM Algorithm Using Continuous-Time HMM

We propose an alternative continuous-time HMM (CT-HMM) EM algorithm that uses the transition probabilities matrices defined as the matrix exponential of transition rate matrices $\mathbf{Q}(t_{ijk})$. In the E-step, Section 2.3.1, the transition probability matrices are replaced with $\boldsymbol{\Gamma}(t_{ijk}) = \exp(\mathbf{Q}(t_{ijk})h_{ijk})$, where

$$\mathbf{Q}(t_{ijk}) = \begin{bmatrix} -\lambda_1(t_{ijk}) & \lambda_1(t_{ijk}) \\ \lambda_2(t_{ijk}) & -\lambda_2(t_{ijk}) \end{bmatrix}.$$

The modified E-step and original M-step (Section 2.3.2) are repeated iteratively until convergence to fit a CT-HMM (Bureau et al., 2003; Liu et al., 2015).

2.5 EM Algorithm Using Logistic Regression HMM

Another alternative method involving discrete-time HMMs modifies the M-step to fit a weighted mixed logistic regression (Altman, 2007; Stoner and Economou, 2020). The E-step

remains the same, but the M-step update is the solution to

$$L(\boldsymbol{\beta}_s, \sigma_s^2, \mathbf{b}_s | \mathbf{A}) = \left[\prod_{i=1}^{n_I} \prod_{j=1}^{n_{iJ}} \prod_{k=1}^{n_{ijk}} [\text{expit}(\eta_s(t_{ijk}))]^{d_s(t_{ijk})} [1 - \text{expit}(\eta_s(t_{ijk}))]^{c_s(t_{ijk})} \right] f(\mathbf{b}_s | \sigma_s^2)$$

which can be obtained using the `lme4` package in R (Bates et al., 2007).

2.6 Competing Methods

One of the primary purpose of HMMs is to impute the state labels $A(t_{ijk})$, so we evaluate competing methods that accomplish the same task. We denote the alternating recurrent event exponential PH model outlined in Section 2.3 as PH-HMM. For our first competing method, we use the CT-HMM described in Section 2.4. We also use the discrete-time mixed effect logistic regression HMM, described in Section 2.5, denoted as DT-HMM.

In addition, we propose a Poisson mixture model (PMM) approach to estimate $\mathbf{u}(t_{ijk})$ directly, treating all of the $Y(t_{ijk})$ as independent random samples using the `flexmix` R package (Leisch, 2004). After we fit our mixture model, we impute *maximum a posteriori* (MAP) estimates, $A^{\text{MAP}}(t_{ijk})$. A well known variation of the HMM is the hidden semi-Markov model (HSMM); they allow for specification of a sojourn time distributions. Each sequence $\mathbf{y}_{ij} = \{Y(t_{ij0}), Y(t_{ij1}), Y(t_{ij2}), \dots\}$, can be fitted with a HSMM (without covariates) using the `hsmm` R package, which uses the Viterbi algorithm to estimate $A^{\text{MAP}}(t_{ijk})$ (Bulla et al., 2010; Viterbi, 1967; Forney, 1973). After we estimate $A^{\text{MAP}}(t_{ijk})$ for each sequence, we then use MAP estimates to calculate $\hat{\mu}_1$ and $\hat{\mu}_2$ across chains.

In order to study coefficients, we compare the coefficients from DT-HMM, CT-HMM, and PH-HMM. In many settings, biomarker $Y(t_{ijk})$ would first be clustered and assigned a state label, then a PH model would be fitted. We replicate this process using PMM and HSMM MAP labels and then fitting the frailty models

$$L(\boldsymbol{\beta}_s, \mathbf{b}_s, \sigma_s^2) = \left(\prod_{i=1}^{n_I} \prod_{j=1}^{n_{iJ}} \prod_{k=1}^{n_{ijk}} [f(h_{ijk} | \lambda_s(t_{ijk}))]^{\mathbb{1}[A^{\text{MAP}}(t_{ij(k-1)})=s, A^{\text{MAP}}(t_{ijk}) \neq s]} \right. \\ \left. \times [S(h_{ijk} | \lambda_s(t_{ijk}))]^{\mathbb{1}[A^{\text{MAP}}(t_{ij(k-1)})=s, A^{\text{MAP}}(t_{ijk})=s]} \right) f(\mathbf{b}_s | \sigma_s^2).$$

3. Results

3.1 Asymptotic Results

The EM algorithm converges and obtains the MLEs $\{\hat{\beta}_s, \hat{\mathbf{b}}_s, \hat{\sigma}_s^2, \hat{\mathbf{c}}_s, \hat{\mathbf{d}}_s\}$, with the final likelihood evaluation being equivalent to weighted exponential frailty models. As a result, we can generalize existing large sample theory asymptotic inference for mixed effect models for our weighted setting, using the exact weights derived in Section 2.3.1 (Schall, 1991; McGilchrist and Aisbett, 1991; Therneau et al., 2003; Bellamy et al., 2004; Abrahantes et al., 2007).

THEOREM 1: *The two state alternating recurrent event exponential PH model with rates, $\lambda_s(t_{ijk}) = \exp(\eta_s(t_{ijk}))$ for $s \in \{1, 2\}$ and latent states, $A(t_{ijk})$, has state transition probabilities $\Pr(A(t_{ij(k-1)}) = s, A(t_{ijk}) \neq s | \eta_s(t_{ijk})) = \text{expit}(\eta_s(t_{ijk}))$ defined by the standard logistic function. Regression coefficients β_s are asymptotically normally distributed $\hat{\beta}_s \xrightarrow{D} N(\beta_s, \Sigma_s)$ where Σ_s are corresponding β_s elements of the inverse observed informations $\mathcal{I}^{-1}(\beta_s, \mathbf{b}_s)$.*

The observed informations are given as

$$\mathcal{I}(\beta_s, \mathbf{b}_s) = \mathbf{U}^\top \left[\frac{-\partial^2 \log L(\beta_s | \mathbf{b}_s, \hat{\mathbf{c}}_s, \hat{\mathbf{d}}_s)}{\partial \eta_s \partial \eta_s^\top} \right] \mathbf{U} + \begin{bmatrix} \mathbf{0} & \mathbf{0} \\ \mathbf{0} & \sigma_s^{-2} \mathbf{I} \end{bmatrix}$$

where $\frac{-\partial^2 \log L(\beta_s | \mathbf{b}_s, \hat{\mathbf{c}}_s, \hat{\mathbf{d}}_s)}{\partial \eta_s \partial \eta_s^\top} = \text{diag}(h_{111}\lambda_s(t_{111}), h_{111}\lambda_s(t_{111}), h_{112}\lambda_s(t_{112}), h_{112}\lambda_s(t_{112}), \dots,$

$h_{ijk}\lambda_s(t_{ijk}), h_{ijk}\lambda_s(t_{ijk}), \dots) \mathbf{W}_s,$

$$\mathbf{U}^\top = \begin{bmatrix} \mathbf{x}(t_{111}) & \mathbf{x}(t_{111}) & \mathbf{x}(t_{112}) & \mathbf{x}(t_{112}) & \dots & \mathbf{x}(t_{t_{ijk}}) & \mathbf{x}(t_{t_{ijk}}) & \dots \\ \mathbf{z}(t_{111}) & \mathbf{z}(t_{111}) & \mathbf{z}(t_{112}) & \mathbf{z}(t_{112}) & \dots & \mathbf{z}(t_{t_{ijk}}) & \mathbf{z}(t_{t_{ijk}}) & \dots \end{bmatrix}$$

and $\mathbf{W}_s = \text{diag}(\hat{d}_s(t_{111}), \hat{c}_s(t_{111}), \hat{d}_s(t_{112}), \hat{c}_s(t_{112}), \dots, \hat{d}_s(t_{ijk}), \hat{c}_s(t_{ijk}), \dots).$

Proof. Proof of Theorem 1. Applying large sample theory results for PH models, we derive the observed information using the weights and augmented data defined in Section 2.3.1, 2.3.2 and Table 1 (McGilchrist and Aisbett, 1991; Abrahantes et al., 2007). Although, Gray (1992)

proposed the asymptotic distribution

$$\left[\hat{\boldsymbol{\beta}}_s^\top, \hat{\mathbf{b}}_s^\top \right]^\top \stackrel{D}{\sim} N \left(\left[\boldsymbol{\beta}_s^\top, \mathbf{b}_s^\top \right]^\top, \mathcal{I}^{-1}(\boldsymbol{\beta}_s, \mathbf{b}_s) \mathbf{U}^\top \left[\frac{-\partial^2 \log L(\boldsymbol{\beta}_s | \mathbf{b}_s, \hat{\mathbf{c}}_s, \hat{\mathbf{d}}_s)}{\partial \eta \partial \eta^\top} \right] \mathbf{U} \mathcal{I}^{-1}(\boldsymbol{\beta}_s, \mathbf{b}_s) \right),$$

the observed information $\mathcal{I}^{-1}(\boldsymbol{\beta}_s, \mathbf{b}_s)$ tends to be used for asymptotic distributions due to it being more conservative (Therneau et al., 2003; Wang et al., 2020).

3.2 Simulation Studies

We sequentially simulate survival data using the `simsurv` package in R, to reflect an alternating survival process (Brilleman et al., 2021). Given a set of coefficients, covariates and censoring time: h_c , `simsurv` returns an event time and survival status, $\delta \in \{1, 0\}$. We use a 24-hour period sine function as our time varying covariate, $x(t) = \sin(2\pi t/24)$ and independently draw censoring times from a Uniform distribution, $h_c \sim U(0, h_{\max})$. We use individual specific random intercepts $\{b_{1i}, b_{2i}\}$ and PH models given as

$$\lambda_1(t_{ik}) = \exp(\mathbf{x}^\top(t_{ik})\boldsymbol{\beta}_1 + \mathbf{z}^\top(t_{ik})\mathbf{b}_1) = \exp(\beta_{10} + \beta_{11}x(t_{ik}) + b_{1i}), \quad \mathbf{b}_1 \sim N(\mathbf{0}, \sigma_1^2 \mathbf{I})$$

$$\lambda_2(t_{ik}) = \exp(\mathbf{x}^\top(t_{ik})\boldsymbol{\beta}_2 + \mathbf{z}^\top(t_{ik})\mathbf{b}_2) = \exp(\beta_{20} + \beta_{21}x(t_{ik}) + b_{2i}), \quad \mathbf{b}_2 \sim N(\mathbf{0}, \sigma_2^2 \mathbf{I})$$

where we suppress the j notation, such that each individual has one HMM. Pseudocode for generating the alternating survival data can be described in Algorithm 1 of the appendix. Once states, $A(t_{ik})$ are obtained, we simulate a state dependent observations from Poisson distributions to complete the simulation of the latent state PH models.

We simulated five cases, with different sets of parameters and compare our four competing methods. First, we evaluated accuracy (number of correctly identified states divided by total number of states) using MAP estimates. Accuracy results for competing methods and simulation parameters can be found in Table 2. When the distribution distance (e.g., symmetric KL divergence) between $f(y(t_{ik})|\mu_1)$ and $f(y(t_{ik})|\mu_2)$ is large, all competing methods have similar performance and are highly accurate, as shown in Cases 1-3. A large distance between $f(y(t_{ik})|\mu_1)$ and $f(y(t_{ik})|\mu_2)$ results in state membership being determined by the $\mathbf{P}(t_{ik})$ matrices and calculations are essentially evaluated as if state memberships were

known. As we close the distance between $f(y(t_{ik})|\mu_1)$ and $f(y(t_{ik})|\mu_2)$, such as Case 5, we found that DT-HMM, CT-HMM and PH-HMM methods are more accurate than PMM and HSMM, because they are able to leverage covariates in modeling state memberships. Case 5 can be viewed as example of misclassified state labels, for which HMMs with covariates excel. However, we found that DT-HMM is the most accurate method, but as a result of model misspecification, we found that overfitting is a concern when using DT-HMM. However, PH-HMM was also more accurate than CT-HMM in all cases and comparable in accuracy to DT-HMM.

Parameter estimates, empirical standard error (ESE) calculated over the replicates, and mean squared error (MSE) can be found in Tables 3 and 4. All competing methods performed well at estimating μ_1 and μ_2 . We found that CT-HMM generally out performed competing methods in the estimation of $\{\beta_s, \sigma_s^2\}$ based on bias then followed by PH-HMM. In Cases 1-3, where the distance between $f(y(t_{ik})|\mu_1)$ and $f(y(t_{ik})|\mu_2)$ is large, DT-HMM, CT-HMM and PH-HMM estimate coefficients close to the true parameter. However, in Case 5, where distance between $f(y(t_{ik})|\mu_1)$ and $f(y(t_{ik})|\mu_2)$ is small, we found the DT-HMM estimates had high variability and unreasonable effect sizes. By maximizing with respect to incorrect likelihood (found in Section 2.5) and compounding the misclassification due to similar $f(y(t_{ik})|\mu_1)$ and $f(y(t_{ik})|\mu_2)$, DT-HMM may be inadequate when robustness is a concern. In conclusion, PH-HMM outperforms CT-HMM with regards to accuracy and outperforms DT-HMM with regards to estimation bias. For these reasons, PH-HMM excels in a variety of situations, making it a reliable method.

[Table 2 about here.]

[Table 3 about here.]

[Table 4 about here.]

3.3 Application: *mHealth Data*

A sample of $n_I = 41$, recruited via the Penn/CHOP Lifespan Brain Institute or through the Outpatient Psychiatry Clinic at the University of Pennsylvania as part of a study of affective instability in youth (Xia et al., 2021). All participants provided informed consent to all study procedures. This study was approved by the University of Pennsylvania Institutional Review Board. For each individual, roughly 3 months of data was collected using the Beiwe platform (Torous et al., 2016). Accelerometer measures (meters per second squared) for x, y and z axes, screen-on events for Android devices and screen-unlock events for iOS (Apple) devices were acquired through the Beiwe platform—we refer to both as “screen-on events” in this manuscript.

However, periods of dormancy, where accelerometer measurements are missing due to user and device related factors such as the phone being powered off or being in airplane mode, requiring accelerometer features to be imputed. By collecting both screen-on events as well as accelerometer data, we are able to construct an accurate model for imputing missing accelerometer data. In our case, there is missing at random (MAR), accelerometer data is missing over a given hour but there are many screen-on events over the same period. On the other hand, there is missing not at random (MNAR), accelerometer data is missing and there are also no screen-on events, then it is likely that the phone was in a state of dormancy. Periods of MNAR have greater probability of missing accelerometer features and are identified using a two state hidden semi-Markov model with Bernoulli state dependent distributions (Bulla et al., 2010). Missing mean acceleration magnitudes from MNAR periods were imputed using the minimum (excluding outliers) of accelerometer features. While missing data assigned to the MAR periods were imputed by regressing accelerometer features on $Y(t_{ijk})$ over all hours where data is completely observed. Periods of consecutive missing acceleration magnitudes over 24 hours constitutes an end to the current sequence and the

start of a new sequence, where the likelihoods of multiple sequences can be multiplied together for parameter estimation as discussed in Section 2.

3.3.1 Estimating Strength of Routine in Youth with Affective Disorders. An important goal in psychiatry studies is modeling regularity of circadian rhythms, especially in rest and activity cycles. In many cases, regularity of a rhythm is defined as the association of time-of-day and state membership. In other words, the effect of hour-of-day on rest and activity state membership models the diurnal rhythm. We assign hour-of-day effects, as normally distributed random intercepts in our HMMs and for each individual we fit PH models $\lambda_s(t_{ijk}) = \exp\left(\mathbf{x}^\top(t_{ijk})\boldsymbol{\beta}_s^{(i)} + \mathbf{z}^\top(t_{ijk})\mathbf{b}_s^{(i)}\right)$, where $\mathbf{b}_s^{(i)} \sim N(\mathbf{0}, \tau_s^{(i)}\mathbf{I})$ and the superscripts denotes parameters specific to individual i . Rates of transition from active-to-rest states are given as $\lambda_1(t_{ijk})$, rates of transition from rest-to-active states are given as $\lambda_2(t_{ijk})$ and an example of HMM outputs can be found in Figure 2. The variances of the random intercepts can be interpreted as a L2 penalty on hour-of-day effects, in addition to being the test statistics in a mixed effect ANOVA, and disappears as $\tau_s^{(i)} \rightarrow \infty$. We quantify the regularity of an individual's rhythm, by summing over the variances $\omega^{(i)} = \tau_1^{(i)} + \tau_2^{(i)}$, where large variances correspond with large hour-of-day effect sizes and greater regularity in diurnal rhythms with an example in Figure 2. For each individual's data, we fit HMMs using competing methods and calculate their $\omega^{(i)}$.

When fitting individual level models, DT-HMM often encounters issues regarding robustness where the $\omega^{(i)}$ exhibit large variability. For some individuals, the distance between $f(y(t_{ijk})|\mu_1^{(i)})$ and $f(y(t_{ijk})|\mu_2^{(i)})$ is small, which is a contributing factor to unstable and bias DT-HMM estimates. As a result, 4 individuals were omitted because their DT-HMM failed to converge. The remaining $\omega^{(i)}$ estimates are derived from individuals where the distance between $f(y(t_{ijk})|\mu_1^{(i)})$ and $f(y(t_{ijk})|\mu_2^{(i)})$ is large and competing methods performed similarly, as shown in Figure 3. These examples highlight the many processes that lead to the complex

nature of mHealth data, resulting in the need for robust models. When considering the high biases of the DT-HMM, we conclude that PMM, HSMM, CT-HMM and PH-HMM are preferable in this application.

[Figure 2 about here.]

[Figure 3 about here.]

3.3.2 Population HMM: Differences Between Operating Systems. Alternatively, we can fit a population model, with random intercepts being specific to each individuals. However, for iOS devices we only have screen-unlock events, i.e., entering in a passcode to unlock the phone. Android devices have screen-on events which occur when the phone screen turns on such as when receiving a message; the phone does not need to be unlocked for the screen to be turned on. Screen-unlock events are less frequent and a subset of screen-on events, causing the counts $Y(t_{ijk})$, to be lower for iOS devices. The relationship between acceleration $x(t_{ijk})$ and $Y(t_{ijk})$, may be weaker in iOS devices. We can test interaction between operating system (OS) and acceleration, while controlling for the interaction with user sex in our regression and other individual effects with random intercepts. Android devices and males serve as baseline in this analysis. For the active-to-rest model: $\lambda_1(t_{ijk})$ and rest-to-active model: $\lambda_2(t_{ijk})$, $\lambda_s(t_{ijk}) = \exp(\mathbf{x}^\top(t_{ijk})\boldsymbol{\beta}_s + \mathbf{z}^\top(t_{ijk})\mathbf{b}_s) = \exp(\beta_{s0} + \beta_{s1}x(t_{ijk}) + \beta_{s2}x(t_{ijk})\text{sex} + \beta_{s3}x(t_{ijk})\text{OS} + b_{si})$, where $\mathbf{b}_s \sim N(\mathbf{0}, \sigma_s^2 \mathbf{I})$ and $\{b_{1i}, b_{2i}\}$ are individual specific random intercepts.

We fit our competing methods and test interaction where estimates can be found in Table 5. For HMM, HSMM, CT-HMM and PH-HMM methods, we have a hazard ratio interpretation of the coefficients and an odds ratio interpretation for the DT-HMM. Standard errors were derived using the asymptotic results from Section 3.1. The standard errors from DT-HMM were calculated with `lme4`, using an approach analogous to Section 3.1.

At a population level, we found that for the active state $\mathbb{E}[y(t_{ijk})|A(t_{ijk}) = 1] \approx 8$ and for rest state $\mathbb{E}[y(t_{ijk})|A(t_{ijk}) = 2] \approx 0.4$. We found that rate of transition from active-

to-rest states are negatively associated with acceleration and rate of transition for rest-to-active states are positively associated with acceleration. These coefficient estimates related to acceleration align with common intuition and are statistically significant ($p < 0.05$) in all competing methods. For HSMM and PMM methods, modeling the MAP estimates first and then combining the estimates to obtain a population level model, does not account for acceleration when imputing state labels and resulted in a poor fit.

We found that in the active-to-rest model, there's no significant interaction between OS and acceleration. In the rest state, $Y(t_{ijk})$ are close to zero regardless of OS, i.e., OS does not contain any useful information related to exiting the active state and transitioning to the rest state. However, in the active state, we know that counts, $Y(t_{ijk})$, are lower for iOS devices. For example, a transition from a rest-to-active state for Android devices may resemble: $Y(t_{ij(k-1)}) = 0$, $Y(t_{ijk}) = 11$, while for iOS, we may observe: $Y(t_{ij(k-1)}) = 0$, $Y(t_{ijk}) = 5$. We were able to detect a significant ($p < 0.05$) interaction term in the rest-to-active model when fitting the PMM, DT-HMM, CT-HMM and PH-HMM. In order to compensate for lower screen-on counts in iOS devices, iOS rest-to-active transitions require a higher magnitude of acceleration to achieve the same transition rate as an Android device. In other words, using the PH-HMM estimates as an example, holding all other covariates constant, the rate of transition from the rest-to-active state for iOS device is $0.95^{x(t_{ijk})} = (\exp(-0.0505))^{x(t_{ijk})}$ that of Android devices. Our results suggest that it is more difficult to discern rest-to-active transitions in iOS devices because of the discrepancy in data collection between operating systems. This finding can be more broadly interpreted as iOS devices having less distinct state memberships.

[Table 5 about here.]

4. Discussion

For a latent state setting, we proposed a method for estimating alternating recurrent event exponential PH model with shared log-normal frailties using the EM algorithm. Our E-step imputations involves a discrete-time HMM using logistic regression transition probabilities with normally distributed random intercepts. The HMM obtain during the E-step of our EM algorithm is alternative method for estimating mixed hidden Markov models (Altman, 2007; Stoner and Economou, 2020; Holsclaw et al., 2017). Random intercepts can be used to account for clustered data, such as data collected from the same individual or hour-of-day periodic effects. We derived asymptotic distributions for the PH regression coefficients and random intercepts, where coefficients have a hazard ratio interpretation akin to the Cox PH model. Our PH-HMM approach is a flexible method for modeling complex mHealth datasets, where time varying or baseline covariates can be incorporated into the PH regression while accounting for latent states. Simulation results and mHealth data analysis suggest that our PH-HMM excels in a variety of situations.

ACKNOWLEDGEMENTS

This work was supported by grants from the National Institute of Mental Health: R01MH116884. Support for data collection was provided by the AE Foundation, R01MH113550 & R01MH107703. The authors wish to thank the Lifespan Informatics & Neuroimaging Center for providing access to the data

REFERENCES

Abrahantes, J. C., Legrand, C., Burzykowski, T., Janssen, P., Ducrocq, V., and Duchateau, L. (2007). Comparison of different estimation procedures for proportional hazards model with random effects. *Computational statistics & data analysis* **51**, 3913–3930.

Alloy, L. B., Boland, E. M., Ng, T. H., Whitehouse, W. G., and Abramson, L. Y. (2015).

Low social rhythm regularity predicts first onset of bipolar spectrum disorders among at-risk individuals with reward hypersensitivity. *Journal of abnormal psychology* **124**, 944.

Altman, R. M. (2007). Mixed hidden markov models: an extension of the hidden markov model to the longitudinal data setting. *Journal of the American Statistical Association* **102**, 201–210.

Balan, T. A. and Putter, H. (2019). frailtyem: An r package for estimating semiparametric shared frailty models. *Journal of Statistical Software* **90**, 1–29.

Bates, D., Sarkar, D., Bates, M. D., and Matrix, L. (2007). The lme4 package. *R package version 2*, 74.

Baum, L. E., Petrie, T., Soules, G., and Weiss, N. (1970). A maximization technique occurring in the statistical analysis of probabilistic functions of markov chains. *The annals of mathematical statistics* **41**, 164–171.

Bellamy, S. L., Li, Y., Ryan, L. M., Lipsitz, S., Canner, M. J., and Wright, R. (2004). Analysis of clustered and interval censored data from a community-based study in asthma. *Statistics in Medicine* **23**, 3607–3621.

Brilleman, S. L., Wolfe, R., Moreno-Betancur, M., and Crowther, M. J. (2021). Simulating survival data using the simsurv r package. *Journal of Statistical Software* **97**, 1–27.

Bulla, J., Bulla, I., and Nenadić, O. (2010). hsmm—an r package for analyzing hidden semi-markov models. *Computational Statistics & Data Analysis* **54**, 611–619.

Bureau, A., Shiboski, S., and Hughes, J. P. (2003). Applications of continuous time hidden markov models to the study of misclassified disease outcomes. *Statistics in medicine* **22**, 441–462.

Dempster, A. P., Laird, N. M., and Rubin, D. B. (1977). Maximum likelihood from incomplete data via the em algorithm. *Journal of the Royal Statistical Society: Series B*

(*Methodological*) **39**, 1–22.

Forney, G. D. (1973). The viterbi algorithm. *Proceedings of the IEEE* **61**, 268–278.

Gray, R. J. (1992). Flexible methods for analyzing survival data using splines, with applications to breast cancer prognosis. *Journal of the American Statistical Association* **87**, 942–951.

Holsclaw, T., Greene, A. M., Robertson, A. W., and Smyth, P. (2017). Bayesian nonhomogeneous markov models via pólya-gamma data augmentation with applications to rainfall modeling. *The Annals of Applied Statistics* **11**, 393–426.

Hothorn, T. (2020). Most likely transformations: The mlt package. *Journal of Statistical Software* **92**, v092–i01.

Hothorn, T., Moest, L., and Buehlmann, P. (2018). Most likely transformations. *Scandinavian Journal of Statistics* **45**, 110–134.

Huang, Q., Cohen, D., Komarzynski, S., Li, X.-M., Innominato, P., Lévi, F., and Finkenstädt, B. (2018). Hidden markov models for monitoring circadian rhythmicity in telemetric activity data. *Journal of The Royal Society Interface* **15**, 20170885.

Hubbard, R., Lange, J., Zhang, Y., Salim, B., Stroud, J., and Inoue, L. (2016). Using semi-markov processes to study timeliness and tests used in the diagnostic evaluation of suspected breast cancer. *Statistics in medicine* **35**, 4980–4993.

Jackson, C. H., Sharples, L. D., Thompson, S. G., Duffy, S. W., and Couto, E. (2003). Multistate markov models for disease progression with classification error. *Journal of the Royal Statistical Society: Series D (The Statistician)* **52**, 193–209.

Jones, S. H., Tai, S., Evershed, K., Knowles, R., and Bentall, R. (2006). Early detection of bipolar disorder: a pilot familial high-risk study of parents with bipolar disorder and their adolescent children. *Bipolar disorders* **8**, 362–372.

Kristensen, K., Nielsen, A., Berg, C. W., Skaug, H., and Bell, B. M. (2016). Tmb: Automatic

differentiation and laplace approximation. *Journal of Statistical Software* **70**,

Lange, T., Dimitrov, S., and Born, J. (2010). Effects of sleep and circadian rhythm on the human immune system. *Annals of the New York Academy of Sciences* **1193**, 48–59.

Langrock, R., Swihart, B. J., Caffo, B. S., Punjabi, N. M., and Crainiceanu, C. M. (2013). Combining hidden markov models for comparing the dynamics of multiple sleep electroencephalograms. *Statistics in medicine* **32**, 3342–3356.

Leisch, F. (2004). Flexmix: A general framework for finite mixture models and latent class regression in r. *Journal of Statistical Software, Articles* **11**, 1–18.

Liu, Y.-Y., Li, S., Li, F., Song, L., and Rehg, J. M. (2015). Efficient learning of continuous-time hidden markov models for disease progression. *Advances in neural information processing systems* **28**, 3599.

Lyall, L. M., Wyse, C. A., Graham, N., Ferguson, A., Lyall, D. M., Cullen, B., Morales, C. A. C., Biello, S. M., Mackay, D., Ward, J., et al. (2018). Association of disrupted circadian rhythmicity with mood disorders, subjective wellbeing, and cognitive function: a cross-sectional study of 91 105 participants from the uk biobank. *The Lancet Psychiatry* **5**, 507–514.

Maruotti, A. and Rocci, R. (2012). A mixed non-homogeneous hidden markov model for categorical data, with application to alcohol consumption. *Statistics in Medicine* **31**, 871–886.

McGilchrist, C. and Aisbett, C. (1991). Regression with frailty in survival analysis. *Biometrics* pages 461–466.

Melo, M. C., Abreu, R. L., Neto, V. B. L., de Bruin, P. F., and de Bruin, V. M. (2017). Chronotype and circadian rhythm in bipolar disorder: a systematic review. *Sleep medicine reviews* **34**, 46–58.

Monaco, J. V., Gorfine, M., and Hsu, L. (2018). General semiparametric shared frailty model:

Estimation and simulation with `frailtyurv`. *Journal of statistical software* **86**,

Monk, T. H., Kupfer, D. J., Frank, E., and Ritenour, A. M. (1991). The social rhythm metric (srm): measuring daily social rhythms over 12 weeks. *Psychiatry research* **36**, 195–207.

Monk, T. K., Flaherty, J. F., Frank, E., Hoskinson, K., and Kupfer, D. J. (1990). The social rhythm metric: An instrument to quantify the daily rhythms of life. *Journal of Nervous and Mental Disease* .

Morris, C. J., Aeschbach, D., and Scheer, F. A. (2012). Circadian system, sleep and endocrinology. *Molecular and cellular endocrinology* **349**, 91–104.

Munda, M., Rotolo, F., Legrand, C., et al. (2012). `parfm`: Parametric frailty models in r. *Journal of Statistical Software* **51**, 1–20.

Pan, S.-T., Kuo, C.-E., Zeng, J.-H., and Liang, S.-F. (2012). A transition-constrained discrete hidden markov model for automatic sleep staging. *Biomedical engineering online* **11**, 1–19.

Qi, J., Yang, P., Waraich, A., Deng, Z., Zhao, Y., and Yang, Y. (2018). Examining sensor-based physical activity recognition and monitoring for healthcare using internet of things: A systematic review. *Journal of biomedical informatics* **87**, 138–153.

Ripatti, S. and Palmgren, J. (2000). Estimation of multivariate frailty models using penalized partial likelihood. *Biometrics* **56**, 1016–1022.

Rondeau, V., Mazroui, Y., and Gonzalez, J. R. (2012). `frailtypack`: an r package for the analysis of correlated survival data with frailty models using penalized likelihood estimation or parametrical estimation. *J Stat Softw* **47**, 1–28.

Schall, R. (1991). Estimation in generalized linear models with random effects. *Biometrika* **78**, 719–727.

Shear, M. K., Randall, J., Monk, T. H., Ritenour, A., Frank, Xin Tu, E., Reynolds, C., and Kupfer, D. J. (1994). Social rhythm in anxiety disorder patients. *Anxiety* **1**, 90–95.

Shinohara, R. T., Sun, Y., and Wang, M.-C. (2018). Alternating event processes during lifetimes: population dynamics and statistical inference. *Lifetime data analysis* **24**, 110–125.

Skarke, C., Lahens, N. F., Rhoades, S. D., Campbell, A., Bittinger, K., Bailey, A., Hoffmann, C., Olson, R. S., Chen, L., Yang, G., et al. (2017). A pilot characterization of the human chronobiome. *Scientific reports* **7**, 1–12.

Song, C., Liu, K., Zhang, X., Chen, L., and Xian, X. (2015). An obstructive sleep apnea detection approach using a discriminative hidden markov model from ecg signals. *IEEE Transactions on Biomedical Engineering* **63**, 1532–1542.

Stoner, O. and Economou, T. (2020). An advanced hidden markov model for hourly rainfall time series. *Computational Statistics & Data Analysis* **152**, 107045.

Tamási, B. and Hothorn, T. (2021). tramme: Mixed-effects transformation models using template model builder.

Therneau, T. M., Grambsch, P. M., and Pankratz, V. S. (2003). Penalized survival models and frailty. *Journal of computational and graphical statistics* **12**, 156–175.

Therneau, T. M. and Lumley, T. (2015). Package ‘survival’. *R Top Doc* **128**, 28–33.

Torous, J., Kiang, M. V., Lorme, J., and Onnela, J.-P. (2016). New tools for new research in psychiatry: a scalable and customizable platform to empower data driven smartphone research. *JMIR mental health* **3**, e16.

Viterbi, A. (1967). Error bounds for convolutional codes and an asymptotically optimum decoding algorithm. *IEEE transactions on Information Theory* **13**, 260–269.

Wang, L., He, K., and Schaubel, D. E. (2020). Penalized survival models for the analysis of alternating recurrent event data. *Biometrics* **76**, 448–459.

Weedon-Fekjær, H., Lindqvist, B. H., Vatten, L. J., Aalen, O. O., and Tretli, S. (2008). Estimating mean sojourn time and screening sensitivity using questionnaire data on

time since previous screening. *Journal of medical screening* **15**, 83–90.

Xia, C. H., Barnett, I., Tapera, T., Cui, Z., Moore, T., Adebimpe, A., Rush, S., Piiwaa, K., Murtha, K., Linguiti, S., et al. (2021). Mobile footprinting: Linking individual distinctiveness in mobility patterns to mood, sleep, and brain functional connectivity. *bioRxiv* .

Zucchini, W., MacDonald, I. L., and Langrock, R. (2017). *Hidden Markov models for time series: an introduction using R*. CRC press.

APPENDIX

Algorithm 1 Algorithm for simulating alternating survival data, $x(t) = \sin(2\pi t/24)$.

```

1:  $\mathbf{b}_1 \leftarrow N(\mathbf{0}, \sigma_1^2 \mathbf{I})$ ,  $\mathbf{b}_2 \leftarrow N(\mathbf{0}, \sigma_2^2 \mathbf{I})$ , data  $\leftarrow \{\}$ 
2: for  $i = 1, 2, \dots, N_I$  do
3:    $r \leftarrow \text{Bernoulli}(0.5)$ 
4:   if  $r = 1$  then
5:      $t_i \leftarrow 0$ ,  $A(t_i) \leftarrow 1$ 
6:   else
7:      $t_i \leftarrow 12$ ,  $A(t_i) \leftarrow 2$ 
8:   end if
9:   append(data,  $\{A(t_i), i\}$ )
10:  for  $k = 1, 2, \dots, N_{iK}$  do
11:    if  $A(t_i) = 1$  then
12:       $h_c \leftarrow U(0, h_{\max})$ 
13:       $\{h, \delta\} \leftarrow \text{simsurv}(\boldsymbol{\beta}_1, x(t_i), b_{1i}, h_c)$ 
14:       $t_i \leftarrow t_i + h$ 
15:      if  $\delta = 1$  then
16:         $A(t_i) = 2$ 
17:      else
18:         $A(t_i) = 1$ 
19:      end if
20:      append(data,  $\{h, A(t_i), x(t_i - h), i\}$ )
21:    else if  $A(t_i) = 2$  then
22:       $h_c \leftarrow U(0, h_{\max})$ 
23:       $\{h, \delta\} \leftarrow \text{simsurv}(\boldsymbol{\beta}_2, x(t_i), b_{2i}, h_c)$ 
24:       $t_i \leftarrow t_i + h$ 
25:      if  $\delta = 1$  then
26:         $A(t_i) = 1$ 
27:      else
28:         $A(t_i) = 2$ 
29:      end if
30:      append(data,  $\{h, A(t_i), x(t_i - h), i\}$ )
31:    end if
32:  end for
33: end for

```

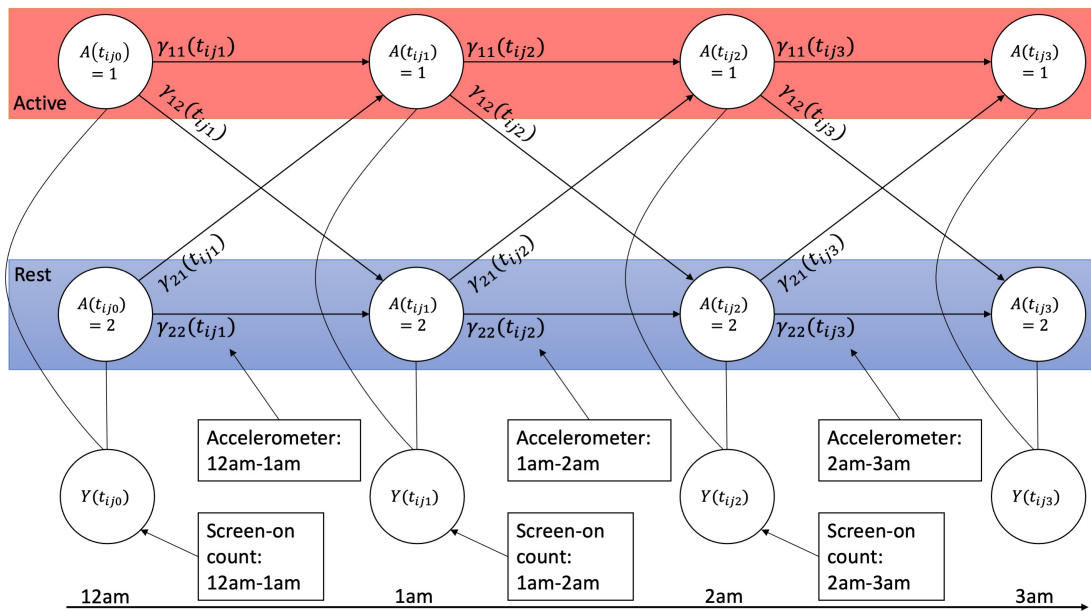


Figure 1. Hidden Markov Model. State dependent distribution of screen-on counts $Y(t_{ijk})$ follow a Poisson distribution. The previous hour's average acceleration magnitudes $\mathbf{x}(t_{ijk})$ are used to estimate state transitions probabilities $\gamma_{qr}(t_{ijk})$.

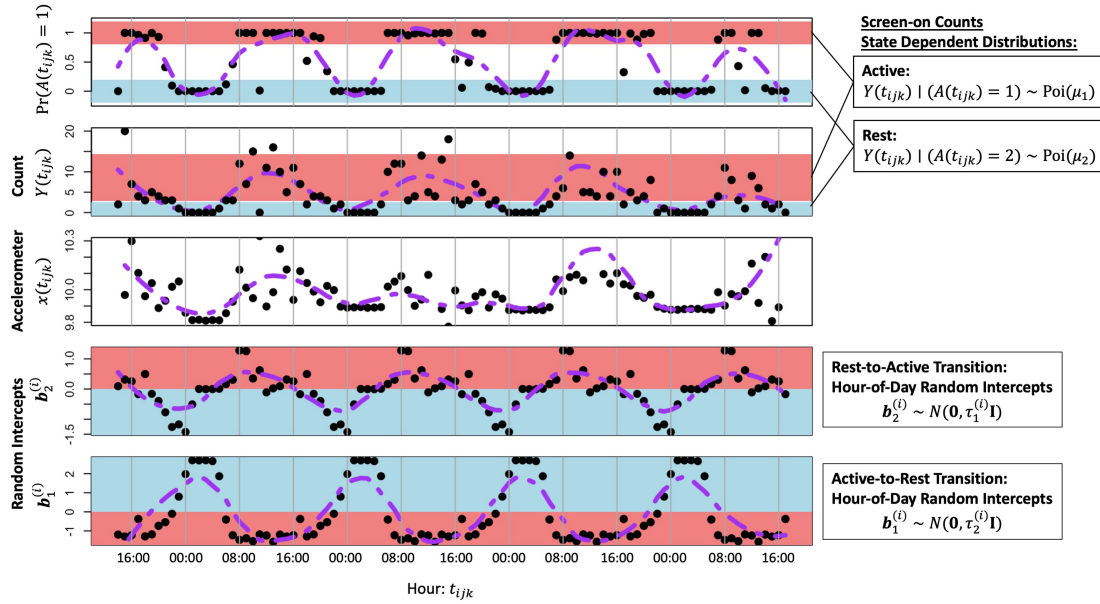


Figure 2. Example of mHealth Data and Fitted HMM. Probabilities of being in the active state, screen-on counts, mean acceleration magnitude, and hour-of-day random intercepts are plotted against time (hours). MAP estimates were calculated using final E-step probabilities $\Pr(A(t_{ijk}) = 1) = \hat{u}_1(t_{ijk})$. Random intercepts capture the diurnal rhythm of active rest cycles, with active states mainly occurring between the hours of 6am-10pm. Large values of $\tau_s^{(i)}$ correspond with a high amplitude in the cyclic diurnal effects.

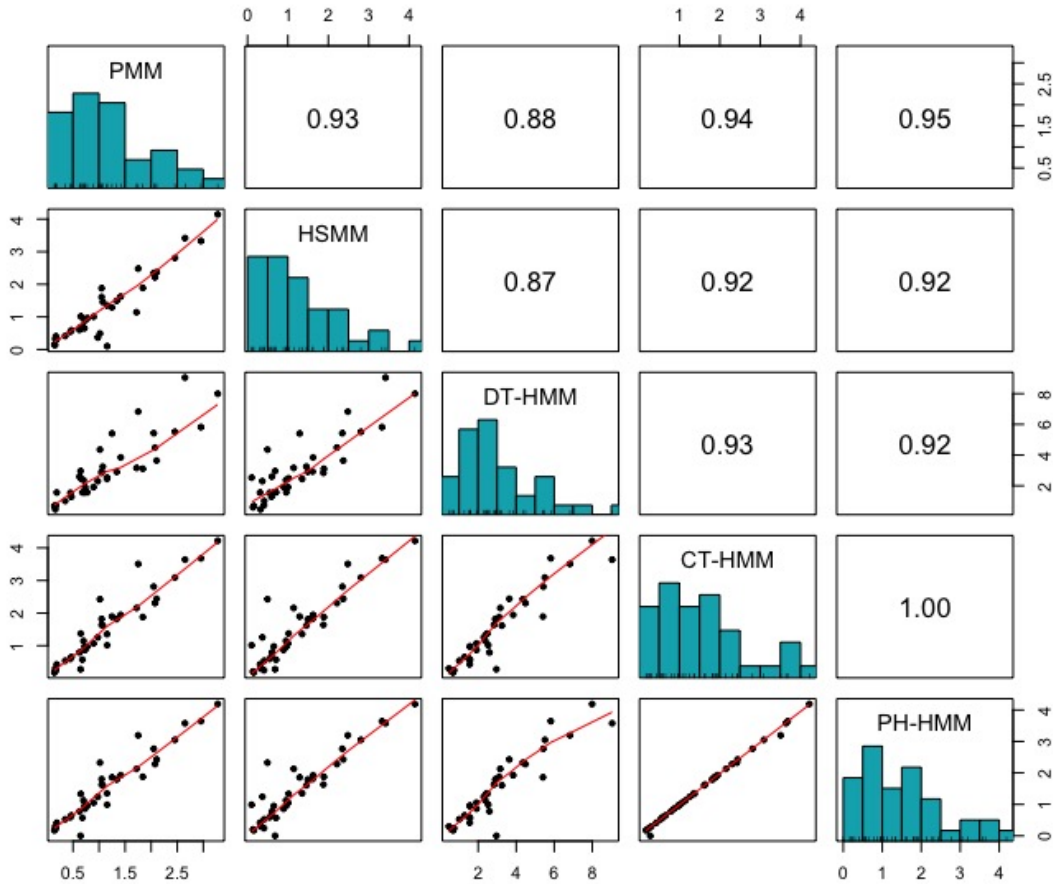


Figure 3. Scatter Plot, Histogram and Pearson Correlation of $\omega^{(i)}$. Each individual was fitted with a competing methods. The variances of their random intercepts across compete methods were calculated and compared using scattered plots and Pearson correlation.

Table 1

Example of Data Augmentation. Each set of covariates and event time is duplicated to be an event and censored outcome. Weights from the E-step $\{\mathbf{d}_1^{(l+1)}, \mathbf{c}_1^{(l+1)}\}$, denotes the probability of an event or censoring. The newly augmented data is fitted with a weighted survival model to obtain $\{\boldsymbol{\beta}_1^{(l+1)}, \mathbf{b}_1^{(l+1)}, \sigma_1^{2(l+1)}\}$. A similar data set can be created to estimate $\{\boldsymbol{\beta}_2^{(l+1)}, \mathbf{b}_2^{(l+1)}, \sigma_2^{2(l+1)}\}$.

event time	random intercept	covariates	$\{\text{event,censored}\} = \{1, 0\}$	weight
h_{111}	$\mathbf{z}^\top(t_{111})$	$\mathbf{x}^\top(t_{111})$	1	$d_1^{(l+1)}(t_{111})$
h_{111}	$\mathbf{z}^\top(t_{111})$	$\mathbf{x}^\top(t_{111})$	0	$c_1^{(l+1)}(t_{111})$
h_{112}	$\mathbf{z}^\top(t_{112})$	$\mathbf{x}^\top(t_{112})$	1	$d_1^{(l+1)}(t_{112})$
h_{112}	$\mathbf{z}^\top(t_{112})$	$\mathbf{x}^\top(t_{112})$	0	$c_1^{(l+1)}(t_{112})$
\vdots	\vdots	\vdots	\vdots	\vdots
h_{ijk}	$\mathbf{z}^\top(t_{ijk})$	$\mathbf{x}^\top(t_{ijk})$	1	$d_1^{(l+1)}(t_{ijk})$
h_{ijk}	$\mathbf{z}^\top(t_{ijk})$	$\mathbf{x}^\top(t_{ijk})$	0	$c_1^{(l+1)}(t_{ijk})$
\vdots	\vdots	\vdots	\vdots	\vdots

Table 2

Simulation: Case Parameters and Accuracy for Competing Methods. Mean accuracy and empirical standard errors based on 500 replicates. Intercepts in every case are set as $\beta_{10} = \beta_{20} = 1$. Max censoring time was set as $h_{\max} = 1$. Each replicate had $n_I = 10$ individuals with $n_{iK} = 100$ state transitions.

Case	Parameters			Methods: mean accuracy (ESE)				
				PMM	HSMM	DT-HMM	CT-HMM	PH-HMM
1	$\beta_{11} = -5$	$\mu_1 = 20$	$\sigma_1^2 = 1$	0.9875(0.0034)	0.9885(0.0053)	0.9941(0.0024)	0.9783(0.0058)	0.993(0.0027)
2	$\beta_{11} = -5$	$\mu_1 = 20$	$\sigma_1^2 = 5$	0.9876(0.0034)	0.9892(0.0072)	0.9952(0.0022)	0.9746(0.0085)	0.9939(0.0025)
3	$\beta_{11} = -2$	$\mu_1 = 20$	$\sigma_1^2 = 1$	0.9877(0.0034)	0.9871(0.0066)	0.9931(0.0026)	0.9566(0.011)	0.9924(0.0029)
4	$\beta_{11} = -5$	$\mu_1 = 15$	$\sigma_1^2 = 1$	0.9473(0.0232)	0.9499(0.0148)	0.9765(0.0049)	0.9254(0.0166)	0.9675(0.006)
5	$\beta_{11} = -5$	$\mu_1 = 10$	$\sigma_1^2 = 1$	0.8202(0.0234)	0.816(0.0343)	0.8944(0.0172)	0.8439(0.0255)	0.8586(0.015)

Table 3

Simulation: Estimates, Standard Errors and Mean Square Errors for β_1 and β_2 . Mean parameter estimates, empirical standard error and mean squared error based on 500 replicates.

Case	Model	[Estimate, ESE, MSE]			
		β_{10}	β_{11}	β_{20}	β_{21}
1	PMM	[0.649, 0.325, 0.229]	[-3.399, 0.638, 2.97]	[0.665, 0.324, 0.217]	[3.471, 0.673, 2.789]
	HSMM	[0.758, 0.319, 0.16]	[-3.949, 0.802, 1.746]	[0.697, 0.309, 0.187]	[3.776, 0.785, 2.114]
	DT-HMM	[0.703, 0.442, 0.283]	[-5.76, 0.626, 0.969]	[0.697, 0.428, 0.275]	[5.778, 0.637, 1.011]
	CT-HMM	[0.74, 0.327, 0.175]	[-4.67, 0.565, 0.427]	[0.787, 0.332, 0.155]	[4.592, 0.524, 0.44]
	PH-HMM	[0.717, 0.274, 0.155]	[-3.421, 0.384, 2.64]	[0.686, 0.277, 0.175]	[3.415, 0.462, 2.726]
2	PMM	[0.729, 0.61, 0.445]	[-3.565, 0.814, 2.72]	[0.734, 0.647, 0.488]	[3.514, 0.811, 2.865]
	HSMM	[0.717, 0.605, 0.446]	[-3.642, 1.064, 2.975]	[0.694, 0.624, 0.483]	[3.489, 1.039, 3.361]
	DT-HMM	[0.706, 0.895, 0.886]	[-5.86, 0.718, 1.253]	[0.722, 0.91, 0.904]	[5.82, 0.731, 1.206]
	CT-HMM	[0.705, 0.674, 0.541]	[-4.402, 0.749, 0.918]	[0.808, 0.689, 0.511]	[4.492, 0.595, 0.612]
	PH-HMM	[0.733, 0.556, 0.38]	[-3.225, 0.609, 3.522]	[0.72, 0.585, 0.42]	[3.229, 0.639, 3.545]
3	PMM	[0.857, 0.308, 0.115]	[-1.662, 0.25, 0.177]	[0.843, 0.324, 0.129]	[4.209, 0.492, 0.868]
	HSMM	[0.808, 0.297, 0.125]	[-1.618, 0.301, 0.236]	[0.88, 0.319, 0.116]	[4.278, 0.505, 0.776]
	DT-HMM	[0.674, 0.421, 0.283]	[-2.362, 0.329, 0.239]	[0.722, 0.445, 0.275]	[5.824, 0.597, 1.036]
	CT-HMM	[0.785, 0.326, 0.152]	[-2.272, 0.23, 0.127]	[0.813, 0.316, 0.135]	[4.351, 0.422, 0.598]
	PH-HMM	[0.916, 0.302, 0.098]	[-1.761, 0.195, 0.095]	[0.838, 0.295, 0.113]	[3.882, 0.405, 1.413]
4	PMM	[0.453, 0.277, 0.376]	[-2.106, 0.417, 8.55]	[0.291, 0.245, 0.562]	[1.939, 0.255, 9.437]
	HSMM	[0.31, 0.271, 0.549]	[-2.442, 0.675, 6.999]	[0.2, 0.266, 0.711]	[2.344, 0.627, 7.444]
	DT-HMM	[0.817, 0.502, 0.285]	[-6.498, 0.966, 3.176]	[0.759, 0.491, 0.299]	[6.308, 0.911, 2.54]
	CT-HMM	[0.066, 0.299, 0.962]	[-3.949, 0.679, 1.564]	[0.247, 0.31, 0.663]	[3.95, 0.604, 1.466]
	PH-HMM	[0.393, 0.202, 0.409]	[-2.066, 0.232, 8.664]	[0.349, 0.212, 0.468]	[2.06, 0.24, 8.702]
5	PMM	[0.312, 0.361, 0.603]	[-0.999, 0.187, 16.046]	[0.172, 0.389, 0.837]	[1.012, 0.134, 15.921]
	HSMM	[-0.816, 0.397, 3.457]	[-1.127, 0.673, 15.453]	[-0.982, 0.442, 4.124]	[1.076, 0.576, 15.729]
	DT-HMM	[7.226, 13.216, 213.129]	[-46.795, 61.181, 5483.78]	[5.396, 9.773, 114.67]	[32.43, 48.095, 3061.684]
	CT-HMM	[-1.431, 0.339, 6.025]	[-3.063, 0.541, 4.043]	[-1.192, 0.338, 4.92]	[3.021, 0.55, 4.217]
	PH-HMM	[0.328, 0.143, 0.472]	[-0.891, 0.135, 16.904]	[0.313, 0.156, 0.497]	[0.897, 0.139, 16.855]

Table 4

Simulation: Estimates, Standard Errors and Mean Square Errors for σ_1^2 , σ_2^2 , μ_1 and μ_2 . Mean parameter estimates, empirical standard error and mean squared error based on 500 replicates.

Case	Model	[Estimate, ESE, MSE]			
		σ_1^2	σ_2^2	μ_1	μ_2
1	PMM	[0.748,0.464,0.278]	[0.755,0.437,0.25]	[20,0.208,0.043]	[5.005,0.107,0.012]
	HSMM	[0.753,0.467,0.279]	[0.742,0.415,0.238]	[20.002,0.232,0.054]	[4.998,0.112,0.012]
	DT-HMM	[1.173,0.757,0.602]	[1.182,0.771,0.626]	[20.001,0.204,0.042]	[5.004,0.102,0.01]
	CT-HMM	[0.773,0.464,0.267]	[0.802,0.452,0.243]	[19.762,0.236,0.112]	[5.049,0.116,0.016]
	PH-HMM	[0.549,0.324,0.309]	[0.592,0.327,0.274]	[20.013,0.204,0.042]	[5.003,0.102,0.01]
2	PMM	[3.112,1.736,6.574]	[3.072,1.831,7.066]	[19.991,0.366,0.134]	[5.014,0.311,0.097]
	HSMM	[3.153,1.849,6.826]	[3.036,1.852,7.282]	[19.979,0.267,0.071]	[4.999,0.127,0.016]
	DT-HMM	[6.003,3.37,12.343]	[5.996,3.469,13.006]	[19.999,0.207,0.043]	[4.999,0.104,0.011]
	CT-HMM	[3.533,1.869,5.641]	[3.772,1.995,5.483]	[19.713,0.271,0.156]	[5.045,0.131,0.019]
	PH-HMM	[2.585,1.42,7.843]	[2.644,1.433,7.599]	[20.009,0.207,0.043]	[4.999,0.103,0.011]
3	PMM	[0.73,0.361,0.203]	[0.985,0.504,0.254]	[19.996,0.216,0.047]	[5.005,0.108,0.012]
	HSMM	[0.763,0.393,0.21]	[0.909,0.484,0.243]	[19.961,0.257,0.067]	[4.974,0.108,0.012]
	DT-HMM	[1.197,0.631,0.437]	[1.178,0.748,0.591]	[20,0.211,0.044]	[5.005,0.105,0.011]
	CT-HMM	[0.922,0.464,0.221]	[0.765,0.422,0.233]	[19.147,0.346,0.847]	[4.901,0.116,0.023]
	PH-HMM	[0.765,0.379,0.199]	[0.723,0.378,0.219]	[20.023,0.21,0.045]	[5.016,0.106,0.011]
4	PMM	[0.356,0.241,0.472]	[0.33,0.22,0.497]	[14.989,0.36,0.129]	[5.015,0.29,0.084]
	HSMM	[0.558,0.369,0.332]	[0.565,0.342,0.306]	[15.029,0.237,0.057]	[5.029,0.196,0.039]
	DT-HMM	[1.496,1.147,1.561]	[1.38,0.978,1.1]	[14.994,0.182,0.033]	[5.001,0.109,0.012]
	CT-HMM	[0.459,0.423,0.471]	[0.528,0.381,0.368]	[14.48,0.269,0.343]	[5.179,0.152,0.055]
	PH-HMM	[0.289,0.202,0.546]	[0.309,0.192,0.514]	[15.052,0.186,0.037]	[4.979,0.111,0.013]
5	PMM	[0.094,0.094,0.829]	[0.099,0.104,0.823]	[10.002,0.308,0.095]	[5.019,0.265,0.07]
	HSMM	[1.474,0.699,0.713]	[1.721,0.836,1.217]	[9.836,0.311,0.124]	[5.198,0.318,0.14]
	DT-HMM	[28.245,99.354,10597.317]	[33.287,350.869,123948.763]	[9.736,0.218,0.117]	[5.225,0.185,0.085]
	CT-HMM	[0.001,0.033,0.998]	[0.003,0.029,0.996]	[9.542,0.244,0.27]	[5.225,0.19,0.087]
	PH-HMM	[0.093,0.123,0.838]	[0.102,0.119,0.82]	[10.097,0.197,0.048]	[4.917,0.145,0.028]

Table 5

Population HMM: Parameter Estimates for Competing Methods. Parameter estimates using EM algorithm and asymptotic standard errors.

Parameters	Methods: Estimate (SE)				
	PMM	HSMM	DT-HMM	CT-HMM	PH-HMM
β_{10}	2.8973(0.8384)	6.0613(1.1132)	10.8254(1.4074)	9.0154(1.2162)	8.5893(1.2036)
β_{11}	-0.4182(0.085)	-0.7601(0.1131)	-1.2431(0.1428)	-1.0828(0.1232)	-1.0395(0.1219)
β_{12}	0.0288(0.0121)	-0.005(0.0179)	0.0379(0.0184)	0.0257(0.0126)	0.0257(0.0126)
β_{13}	0.007(0.0124)	-0.0246(0.0185)	0.0052(0.0189)	0.0054(0.013)	0.005(0.0129)
σ_1^2	0.1099	0.2514	0.2585	0.1171	0.116
β_{20}	-6.6357(0.3846)	-5.5955(0.5448)	-16.2898(1.3782)	-6.0404(0.4941)	-5.9631(0.5029)
β_{21}	0.5359(0.0405)	0.4094(0.0563)	1.528(0.1401)	0.4671(0.0512)	0.4599(0.0521)
β_{22}	-0.0278(0.019)	-0.0179(0.0191)	-0.0441(0.0203)	-0.0357(0.0183)	-0.0355(0.0183)
β_{23}	-0.0431(0.0191)	-0.0292(0.0196)	-0.0541(0.0208)	-0.0503(0.0187)	-0.0505(0.0188)
σ_2^2	0.2802	0.2877	0.321	0.2631	0.2634
μ_1	8.5321	6.9505	8.0866	8.0251	8.0114
μ_2	0.5238	0.3554	0.4263	0.4195	0.4153